

# Mg-based composites as effective materials for storage and generation of hydrogen for FC applications

D. Korablov<sup>1</sup>, O. Bezdorozhev<sup>1</sup>, V. Yartys<sup>2</sup>, Yu. Solonin<sup>1</sup>

<sup>1</sup>Frantsevich Institute for Problems of Materials Science, NASU, Kyiv, Ukraine

<sup>2</sup>Institute for Energy Technology, Kjeller, Norway

Today, hydrogen is considered as an ideal choice for storing and carrying energy produced by renewable power sources since it is renewable, eco-friendly and has a high energy density. However, due to the low hydrogen storage capacity, high cost and safety issues of the conventional storage methods, several challenges need to be resolved to effectively use hydrogen in mobile applications. Solid-state hydrogen storage in atomic form in hydrides is a promising method of storage for this purpose, particularly because a double amount of hydrogen can be produced via hydrolysis reaction of chemically active hydrides. Among the metal hydrides, magnesium hydride ( $MgH_2$ ) is considered to be one of the most attractive candidates. However, the hydrolysis reaction is rapidly hindered by the passivation layer formed on the surface of  $MgH_2$ . In order to improve  $MgH_2$  hydrolysis efficiency various approaches have been applied. This paper reviews recent progress on the modifications of  $MgH_2$ -based materials by adding different type of additives, including metals, oxides, hydroxides, halides and surfactants. The introduced additives possess different catalytic properties due to their intrinsic physical and chemical characteristics, and therefore can strongly influence the hydrolysis reaction of  $MgH_2$ . The most promising results were obtained for various salt additives showing that the reaction rate depends mostly on the additive type rather than on concentration. The effect of preparation technique on the hydrolysis of  $MgH_2 - MgCl_2$  composites was studied in detail. The obtained results indicate that efficient hydrolysis performance can be achieved by ball milling of the freshly synthesized  $MgH_2$  with 5 wt.%  $MgCl_2$  and 1 wt.%  $TiC-2TiB_2$  additives. The combination of the applied approaches exhibited a notable synergistic effect on the hydrogen generation.

**Keywords:** Hydrogen generation, Hydrogen accumulation, Mg-based composites, Renewable power sources, Hydrolysis

## 1. Introduction

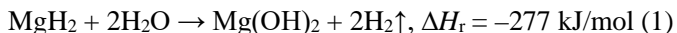
Increase of the energy consumption and challenges appearing from the environmental pollution issues (such as global warming and associated climate changes) caused by industrialization, urbanization and extensive consumption of non-renewable fossil fuels triggered a huge interest to the exploration of green and renewable energy sources. Renewable energy technologies will play a key role in the transition from the fossil fuel economy toward a "green" energy system [1, 2]. In this context, hydrogen is considered as an ideal choice for future clean energy production because of its high energy density, environmental friendliness and renewability. However, the main challenges in the transition to the hydrogen energy are the issues associated with its production, storage and delivery.

Although hydrogen is abundant in nature element, it is primarily bound to other elements forming very stable compounds (water, hydrocarbons), and thus, hydrogen production always requires energy inputs. Hydrogen can be extracted from fossil fuels, biomass, and water by using economically efficient techniques, for example, electricity obtained from renewable energy sources. Although a significant progress has been achieved in hydrogen production, development of the effective methods of hydrogen storage remains on the agenda since the existing solutions have some limitations. Hydrogen can be stored in gaseous state, liquid state or in solid metal hydrides [3, 4]. Conventional high pressure gas storage system has maneuverability, but is costly, requires a high energy consumption and transportation costs, while liquid hydrogen-based storage systems require use of cryotemperatures, show a high energy consumption and cost, thus increasing the requirements to the features of the required equipment. Compared with these storage systems, the solid-state hydrogen storage has the potential to achieve high energy efficiency, good cycle stability, high safety and low cost for use in hydrogen storage applications [3].

On the other hand, solid-state hydrogen storage is characterized by a rather low gravimetric energy density even while considering the material itself only instead of the mass of the system [5]. Moreover, in solid-state storage systems hydrogen is released in an endothermic reaction, which

limits the rates of hydrogen supply due to the poor thermal conductivity of hydrides. Solid-state hydrogen storage is based on metal hydrides, intermetallic hydrides, and complex hydrides showing a variable performance at various P-T conditions [6].

Among the metal hydrides, MgH<sub>2</sub>-based materials have attracted considerable attention due to the high natural abundance of magnesium, low cost of magnesium metal, good reversibility of hydrogen uptake and release, light weight, and high hydrogen storage capacity [3, 4, 7–9]. Pure magnesium can absorb hydrogen up to 7.6 wt.%, but has a slow absorption/desorption kinetics. High thermal stability of MgH<sub>2</sub> and its easy surface oxidation in air impede its applications. To overcome these limitations, a significant amount of research has been performed on the nanosizing, nanoconfinement, alloying, and modifying with intermetallic compounds, metal oxides, halides, carbon materials, hydrides, borohydrides, their mixtures, etc. [7–12]. Although much progress has been achieved, their performance still cannot meet requirements for mobile applications. In this context, small portable applications attract interest as they could be used to power a fuel cell coupled to a hydrogen source that provides the H<sub>2</sub> fuel on demand. An attractive way to implement this concept is to take advantage of the hydrolysis of various metals (e.g., Al-based alloys, Mg [13, 14]) and metal hydrides (e.g., LiH, LiBH<sub>4</sub>, NaBH<sub>4</sub>, MgH<sub>2</sub> [5, 15]). Compared with other hydrolysis materials, MgH<sub>2</sub>-based materials have promising features [16] due to the high hydrogen yield (15.2 wt.% H<sub>2</sub>, when hydrolyzed), relatively low cost, and a formation of the environmentally friendly by-product Mg(OH)<sub>2</sub> [5, 17]. The chemical reaction between MgH<sub>2</sub> and H<sub>2</sub>O is as follows (1):



The hydrolysis reaction of MgH<sub>2</sub> can proceed spontaneously in contact with water at room temperature. However, the hydrolysis of MgH<sub>2</sub> immediately terminates due to the formation of a passive Mg(OH)<sub>2</sub> layer on the MgH<sub>2</sub> surface. The passivation layer prevents the diffusion of water molecules toward the surface of MgH<sub>2</sub>, causing the hydrolysis to rapidly stop, while the initial reaction rate is high. Magnesium hydroxide has a poor solubility in water (1.22 mg/100 mL at 20 °C) [6], and the maximum

reaction yield after 1 h does not exceed 30 % [5]. Eliminating the cladding effect of magnesium hydroxide passivation layer on  $\text{MgH}_2$  has become an urgent problem to be solved to increase the hydrogen yield by hydrolysis [18].

To address this issue, various approaches, such as nanostructuring, the addition of acids, alkali metals, salts, inert additives at ambient conditions or when under heating, ultrasonic irradiation, stirring, were tested to achieve higher hydrogen yield [5, 14, 16, 17, 19]. These approaches improve the hydrolysis performance, while their combination exhibits the notable synergistic effects. However, some aspects of hydrolysis of  $\text{MgH}_2$ -based materials require further investigations and optimization. The hydrolysis reaction is strongly influenced by the characteristics of the hydrolyzed materials, solution composition as well as by the preparation procedure. Since it is possible to improve the hydrolysis of  $\text{MgH}_2$ -based materials by optimizing their preparation procedure, we studied its effect on the hydrolysis performance of  $\text{MgH}_2 + 5 \text{ wt.}\% \text{ MgCl}_2$ . Moreover, in this study, we summarized the recent advances in the hydrolysis of the  $\text{MgH}_2$ -based materials.

## **2. Recent trends in the hydrolysis of $\text{MgH}_2$ -based materials**

### **2.1. Hydrolysis of $\text{MgH}_2$ -based materials with metal additives**

Several metals and their hydrides have been tried as doping catalysts and/or as the components involved into the reaction in order to change the hydrolysis kinetics of Mg-based materials. The ball milling of Mg or  $\text{MgH}_2$  with catalytic metal agents offers advantages of synergy between nanostructuring and alloying resulting in the synthesis of new products with improved hydrogen generation properties, as was shown, for example, in the case of  $\text{Mg}_3\text{RE}$  [20, 21], Mg–Al [22] and Mg–Ca alloying systems [23].

In this connection, the work of Awad et al. [17] should be mentioned, who studied the effect of transition metals such as Ni, Fe and Al on the hydrolysis performance of Mg-based materials in a 3.5 wt.% NaCl solution. They found that the presence of metal elements improves the efficiency of the ball milling process by decreasing the particle size and

by creating more microstructural defects which leads to a more efficient synthesis of  $\text{MgH}_2$ . As the result, the weight content of  $\text{MgH}_2$  after 5 h of ball milling was 4% and 24% for Mg – 10 wt.% Ni and Mg – 10 wt.% Fe mixtures, respectively, while no  $\text{MgH}_2$  was detected in the case of Mg – 10 wt.% Al mixture. The composites with Fe, Ni and Al released respectively 81%, 97% and 45% of the theoretical hydrogen yield after 30 min. The improved hydrogen yield of composites with Ni and Fe is attributed to the formation of micro-galvanic cells between Mg and transition metals that facilitate the corrosion of Mg. However,  $\text{MgH}_2$  formed on the surface of the particles limits the galvanic connection and corrosion processes due to the low electrical conductivity of the hydride (band gap of 5 eV), which explains low  $\text{H}_2$  yield in case of Fe addition in comparison to Ni one.

Recently, Mao et al. [24] studied the solid-solution effect of 10 wt.% In and 5 wt.% Ag on the hydrogen storage and hydrolysis properties of Mg. They found that upon hydrogenation of the Mg(In) or Mg(Ag) solid-solution,  $\text{MgH}_2$ -MgIn or  $\text{MgH}_2$ -MgAg composites are formed. The obtained materials show improved hydrogen sorption performances as well as hydrolysis behavior. Particularly, after hydrolysis at 25 °C for 500 s,  $\text{MgH}_2$ -MgIn releases 895.2 mL/g  $\text{H}_2$  that is relatively higher than in the system  $\text{MgH}_2$ -MgAg (733.6 mL/g) and also for the individual  $\text{MgH}_2$  (631.1 mL/g). This corresponds to about 91%, 92% and 64% hydrogen release for the hydrogenated  $\text{MgH}_2$ -MgIn,  $\text{MgH}_2$ -MgAg and  $\text{MgH}_2$ , respectively. The enhanced hydrolysis performance of the samples the authors attributed to the evenly dispersed nano MgIn or MgAg intermetallics that not only serve as dispersants controlling the growth of  $\text{MgH}_2$  particles and enhancing the contact area with  $\text{MgCl}_2$  aqueous solution but also act as reactants directly participating in the hydrolysis reaction.

The effect of adding 5–20 wt.% Ge on the hydrolysis of  $\text{MgH}_2$  was investigated in [25]. In such a case, Ge does not interact with  $\text{MgH}_2$  under the ball milling conditions, but forms  $\text{Mg}_2\text{Ge}$  at  $T > 370$  °C. By studying the hydrolysis of  $\text{MgH}_2$ -Ge composites, it was found that the unmodified  $\text{MgH}_2$  exhibits 1.5–2.5 slower  $\text{H}_2$  generation rates than  $\text{MgH}_2$ -Ge materials even in concentrated (50 wt.%) acetic acid. Introduction of 5–20 wt.% Ge significantly improves the hydrolysis performance of  $\text{MgH}_2$  when about

100 % H<sub>2</sub> yield is observed after less than 1 minute at the optimal hydrolysis conditions (30–50 wt.% solution of acetic or citric acid at T=30 °C). It should be noted that the hydrogen evolution kinetics was faster for the acetic acid probably due to the different pKa values of the acetic and citric acids related to their reactivity with the substrate. The highest hydrogen generation capacity (~1.56 NL/g) was achieved for the composites containing 5 wt.% Ge, while the increase of Ge content to 20 wt.% results in the lowering of the amount of the generated H<sub>2</sub> to 1.26 NL/g. The improvements of hydrolysis reaction by the addition of Ge, authors explained by the increase of the reaction surface area, number of nucleation centers and creation of micro-galvanic cells between Mg and Ge. The variation of ball milling time from 1 h to 10 h and hydrolysis temperature from 30 °C to 50 °C does not significantly change the kinetics of hydrolysis.

Ma et al. [26] investigated the hydrolysis properties of MgH<sub>2</sub>-CaH<sub>2</sub> composites in-situ hydrogenated using the CaMg<sub>2</sub> and CaMg<sub>1.9</sub>Ni<sub>0.1</sub> intermetallic alloys. The XRD analysis revealed that after the hydrogenation CaMg<sub>2</sub> predominantly formed MgH<sub>2</sub> and Ca<sub>4</sub>Mg<sub>3</sub>H<sub>14</sub>, while CaMg<sub>2</sub>, MgNi<sub>2</sub> and Ca<sub>5</sub>Mg<sub>9</sub>H<sub>28</sub> phases appeared after the hydrogenation of CaMg<sub>1.9</sub>Ni<sub>0.1</sub> alloy. Ma et al. [26] found that after 12 min of hydrolysis in pure water the hydrogen yield of H-CaMg<sub>1.9</sub>Ni<sub>0.1</sub> (1053 mL/g) was higher than that of H-CaMg<sub>2</sub> (800 mL/g). However, the hydrolysis kinetics of H-CaMg<sub>1.9</sub>Ni<sub>0.1</sub> is sluggish during the first 5 minutes of the reaction. A possible reason for the improved hydrolysis performance of H-CaMg<sub>1.9</sub>Ni<sub>0.1</sub> is in a catalytic effect of MgNi<sub>2</sub>, which promotes the hydrolysis reaction around the interface region.

In order to improve the hydrolysis performance of Mg-based materials, Jiang et al. [27] prepared MgLi hydrides via the milling and hydrogenation of MgLi alloy. The prepared hydrides mostly consisted of Mg(Li)H<sub>2</sub> and Mg with small amounts of MgO and Li<sub>2</sub>O. When hydrolyzed, the samples can produce 1542 mL/g and 1773 mL/g (15.8 wt.%) hydrogen after 5 min and 30 min of reaction with MgCl<sub>2</sub> water solution, respectively. The initial rapid hydrogen generation is mainly the result of the violent reaction of LiH with water, while the following

reaction happens in a slow pace during the destabilization of the  $\text{Mg}(\text{OH})_2$  layer on the  $\text{MgH}_2$  and Mg particles by chloride ions.

In the study by Naseem et al. [28],  $\text{Al}_{12}\text{Mg}_{17}$  alloy was used to obtain a mixture of  $\text{MgH}_2$  and Al, which was milled with 1.5 wt.% Mo and 3.5 wt.%  $\text{B}_2\text{O}_3$  as grinding agents. The maximum conversion yield of 97.9% and the hydrogen generation of 1420.2 mL/g were observed for the prepared composite after hydrolysis in a 1 M  $\text{AlCl}_3$  solution for 50 min. The hydrolysis process of  $\text{MgH}_2$  and Al is catalyzed by Mo and  $\text{B}_2\text{O}_3$  additives, where Mo forms a galvanic cell with Al accelerating its dissolution, and  $\text{B}_2\text{O}_3$  forms boric acid, which along with  $\text{AlCl}_3$  facilitates the dissolution of hydroxide layers on the  $\text{MgH}_2$  and Al particles.

## 2.2. Hydrolysis of $\text{MgH}_2$ -based materials with oxide and hydroxide additives

The role of addition of oxide on the hydrolysis performance of  $\text{MgH}_2$  was firstly investigated by Hong et al. [29], who showed that the milling of  $\text{MgH}_2$  with 5 wt.% MgO significantly increases the reactivity of the  $\text{MgH}_2$  particles towards water due to the creation of numerous defects and clean surfaces along with the particle size refining. This study was followed by Awad et al. [17], who also showed that milling Mg with  $\text{V}_2\text{O}_5$  and  $\text{Nb}_2\text{O}_5$  leads to the higher density of defects, fracture and cracking of Mg/ $\text{MgH}_2$  particles. Moreover, Mg-based materials with  $\text{Nb}_2\text{O}_5$  additive were found to be more effective in terms of hydrolysis than with  $\text{V}_2\text{O}_5$  or transition metal additives.

Hydrolysis behavior of core-shell structured Mg- $\text{MO}_x$  (M=Al, Ti and Fe) nanocomposites prepared by arc plasma method and subsequent hydrogenation was studied in [30]. The synthesized and hydrogenated materials mostly contained  $\text{MgH}_2$  with a low fraction of unreacted Mg and MgO, Fe,  $\text{MgAl}_2\text{O}_4$  that formed during the arc plasma evaporation. The hydrogen yields by performing hydrolysis in 0.1M  $\text{MgCl}_2$  aqueous solution of the hydrogenated and passivated Mg- $\text{Al}_2\text{O}_3$ , Mg- $\text{TiO}_2$ , Mg- $\text{Fe}_2\text{O}_3$  composites are 1503 mL/g (93.3%), 1525 mL/g (93.7%) and 1240 mL/g (85%), respectively, which are much higher than that for the passivated pure Mg (1167 mL/g, 77.7%). Thus, the hydrolysis reaction of core-shell nanostructured  $\text{MgH}_2$ - $\text{MO}_x$  is dramatically facilitated. Among all studied

composite powders, the passivated Mg–TiO<sub>2</sub> after the hydrogenation shows the best hydrolysis performances. This is due to the amphoteric nature of TiO<sub>2</sub> that locally at the surface of MgH<sub>2</sub> creates an acidic environment when it contacts with water (2). The formed acidic sites destroy the Mg(OH)<sub>2</sub> passive layer and, along with the created internal defects, promote the hydrolysis of MgH<sub>2</sub>.



In the case of hydrogenated Mg–Fe<sub>2</sub>O<sub>3</sub>, the in-situ generated Fe during arc plasma evaporation forms micro galvanic cells, which accelerate the corrosion of MgH<sub>2</sub>. However, the hydrogen yield of hydrogenated Mg–Fe<sub>2</sub>O<sub>3</sub> is relatively low due to the fact that the addition of Fe<sub>2</sub>O<sub>3</sub> reduces the hydrogen absorption content of Mg.

Yang et al. [31] studied the hydrolysis performance of MgH<sub>2</sub>–5wt.%C and MgH<sub>2</sub>–5wt.%C–5wt.%Fe<sub>2</sub>O<sub>3</sub> composites in municipal drinking water. After 5 min of hydrolysis at 353 K, the hydrogen yield of pure MgH<sub>2</sub>, MgH<sub>2</sub>–C, and MgH<sub>2</sub>–C–Fe<sub>2</sub>O<sub>3</sub> was found to be 202 mL/g, 416 mL/g, and 468 mL/g, while the conversion rate reached 19.3%, 52.5%, and 62.8%, respectively, after 60 min of reaction. It can be seen that addition of graphite and Fe<sub>2</sub>O<sub>3</sub> significantly improved the hydrolysis performance of MgH<sub>2</sub>. The authors attributed this synergistic effect to the lubricating properties of graphite that effectively reduces the agglomeration and size of magnesium particles, while Fe<sub>2</sub>O<sub>3</sub> can further reduce the particle size of MgH<sub>2</sub> and may have a catalytic effect on the hydrolysis reaction.

Recently, Zhou et al. [32] systematically investigated the catalytic activity of typical oxides (MgO, Al<sub>2</sub>O<sub>3</sub>, CaO), hydroxides (Mg(OH)<sub>2</sub>, Al(OH)<sub>3</sub>, Ca(OH)<sub>2</sub>) and chlorides on the hydrolysis reaction of MgH<sub>2</sub> with water. They found that MgH<sub>2</sub>–10 wt.%(MgO, Al<sub>2</sub>O<sub>3</sub> or CaO) composites deliver only 433.0 mL/g, 432.4 mL/g and 421.0 mL/g hydrogen, respectively, within 60 min as compared to that of pure MgH<sub>2</sub> (377 mL/g). In this case oxides play the role of grinding aid that more effectively reduces the particle size of MgH<sub>2</sub>. However, such modification is limited by the milling efficiency. When 10 wt.% Mg(OH)<sub>2</sub>, Al(OH)<sub>3</sub>, and Ca(OH)<sub>2</sub> is introduced, the hydrogen generation performances are slightly

decreased, delivering 407.2 mL/g, 357.3 mL/g, and 340.0 mL/g hydrogen, respectively. Here, the performance is influenced by the solubility of the hydroxides in water and the corresponding solutions produce more OH<sup>-</sup> ions, which favors the formation of Mg(OH)<sub>2</sub> at the surface of MgH<sub>2</sub>.

### 2.3. Hydrolysis of MgH<sub>2</sub>-based materials with halide additives

Alternatively to the use of the acids, the chlorides are usually utilized as agents to create more aggressive medium to enhance the hydrolysis of MgH<sub>2</sub> and inhibit the formation of Mg(OH)<sub>2</sub>. Recently, Zhou et al. [32] studied the effect of a series of 10 wt.% salt additives, including CoCl<sub>2</sub>, NiCl<sub>2</sub>, CuCl<sub>2</sub>, MgCl<sub>2</sub>, CaCl<sub>2</sub>, NaCl, and KCl, on the hydrolysis reaction of MgH<sub>2</sub> with water. The 10 wt.% NaCl, KCl or CaCl<sub>2</sub> containing MgH<sub>2</sub> composites exhibit enhanced hydrolysis properties (540.1 mL/g, 590.2 mL/g and 604.5 mL/g H<sub>2</sub>, respectively) compared to that of MgH<sub>2</sub> (377 mL/g). Both the hydrogen generation yield and hydrolysis kinetics of MgH<sub>2</sub> get further dramatically improved when catalyzed by CoCl<sub>2</sub>, NiCl<sub>2</sub>, CuCl<sub>2</sub> or MgCl<sub>2</sub>, of which the solid-liquid systems deliver 1481.7 mL/g, 1496.1 mL/g, 1472.1 mL/g and 1554.6 mL/g H<sub>2</sub> in 60 min, respectively. The introduced chlorides show different catalytic properties due to their intrinsic physical characteristics. The aqueous solution has a neutral pH value when the neutral chloride (i.e. NaCl, KCl) is completely soluble in water. However, the cation ions from the acidic chloride (i.e. CoCl<sub>2</sub>, NiCl<sub>2</sub>, CuCl<sub>2</sub>, MgCl<sub>2</sub>) have a trend to dissociate water with the generation of more H<sup>+</sup>, therefore making the corresponding aqueous solution weakly acidic. The authors state that Cl<sup>-</sup> ions present in the aqueous solutions destroy the dense Mg(OH)<sub>2</sub> layer via a pitting corrosion, when introducing neutral chlorides only. However, both the anions (Cl<sup>-</sup>) and cations (i.e. Co<sup>2+</sup>, Ni<sup>2+</sup>, Mg<sup>2+</sup>, Cu<sup>2+</sup>) derived from the acid chloride aqueous solution are able to attack the dense Mg(OH)<sub>2</sub> layer via pitting corrosion and H<sup>+</sup> corrosion, respectively. That is why the neutral chloride can promote the hydrolysis reaction at an early stage only while the acidic chloride can increase the hydrolysis performance during the whole process.

In the same study [32] Zhou et al. investigated the effect of milling duration (0–5 h), amounts of additives (3–15 wt.% CoCl<sub>2</sub>) and the way of

introducing solute on the hydrolysis of  $\text{MgH}_2 - 10 \text{ wt.}\% \text{ CoCl}_2$ . They found that 3–5 h-milled composites provide the highest hydrogen yield due to the reduced particle sizes, from  $5.8 \mu\text{m}$  to  $0.7\text{--}0.9 \mu\text{m}$ . The optimal amount of  $\text{CoCl}_2$  was 10 wt.% as the hydrolysis performance at 15 wt.%  $\text{CoCl}_2$  remained unchanged. Comparing the hydrolysis performance of  $\text{MgH}_2 - \text{CoCl}_2$  and  $\text{MgH}_2$  hydrolyzed in  $\text{CoCl}_2$  aqueous solution, where  $\text{CoCl}_2$  content in the two hydrolysis systems was kept at the same level, it was observed that the kinetics of hydrolysis improves with the increasing  $\text{CoCl}_2$  concentration. However, the system demonstrated advanced hydrogen generation kinetics and capacity in the former case for the same amount of introduced  $\text{CoCl}_2$ . This is probably due to the higher local concentration of  $\text{CoCl}_2$  around  $\text{MgH}_2$  after the milling process. Authors concluded that the effect of the solution ions is proportional to the ions concentration in the solution, independently of the way of introducing a solute.

A systematic study of the effect of various halides on the hydrolysis of  $\text{MgH}_2$  was performed by Sevastyanova et al. [33], who studied  $\text{NH}_4\text{F}$ ,  $\text{NH}_4\text{Cl}$ ,  $\text{NH}_4\text{Br}$ ,  $\text{NH}_4\text{I}$ ,  $\text{NaCl}$ ,  $\text{KCl}$ ,  $\text{LiCl}$ ,  $\text{FeCl}_3$ ,  $\text{MgBr}_2$ ,  $\text{MgSO}_4$ ,  $\text{MgCl}_2 \cdot 6\text{H}_2\text{O}$ ,  $\text{CaCl}_2 \cdot 2\text{H}_2\text{O}$ ,  $\text{CoCl}_2 \cdot 2\text{H}_2\text{O}$ ,  $\text{NiCl}_2 \cdot 6\text{H}_2\text{O}$ ,  $\text{CuCl}_2 \cdot 2\text{H}_2\text{O}$  compounds to prepare aqueous solutions. They found that the hydrolysis process of  $\text{MgH}_2$  accelerates in salt solutions, but the reaction rates depend more on the type of the salt rather than on the solution amount (see Table 1). Among tested salts, the most effective catalysts were ammonium chloride and bromide, as well as magnesium chloride, albeit with slightly different reaction rates, pointing out at the differences in the reaction mechanism. In the case of binary salt mixtures, the highest reaction rate and hydrogen yield were observed for  $\text{MgCl}_2 + \text{NH}_4\text{Cl}$ . The authors emphasize that pH value is not the main factor determining the reaction, and ionic strength of the solution should also be considered since the combination of two various salts leads to a marked hydrolysis improvement.

Table 1 – Hydrogen yield in the  $\text{MgH}_2$  hydrolysis reaction for the various salt solutions [33]

Salt	Salt concentration, mol/L (solution volume, mL)	Theoretical H <sub>2</sub> yield over 300 min, %	Theoretical maximum H <sub>2</sub> production, % (reaction completion time, h)
1	2	3	4
LiCl	0.85 (2)	57	78 (30)
NaCl	0.85 (2)	46	85 (57)
NaCl	0.85 (1)	49	100 (40)
KCl	0.85 (2)	66	94 (26)
NH <sub>4</sub> F	0.85 (2)	16	21 (8)
NH <sub>4</sub> Cl	0.85 (0.5)	100	100 (4)
NH <sub>4</sub> Cl	0.85 (1)	100	100 (3)
NH <sub>4</sub> Cl	0.85 (2)	100	100 (4)
NH <sub>4</sub> Cl	0.85 (5)	82	82 (3)
NH <sub>4</sub> Br	0.85 (2)	100	100 (4)
NH <sub>4</sub> I	0.85 (2)	92	94 (6)
MgCl <sub>2</sub>	0.45 (0.5)	99	99 (7)
MgCl <sub>2</sub>	0.45 (1)	97	97 (6)
MgCl <sub>2</sub>	0.45 (2)	90	90 (5)
MgBr <sub>2</sub>	0.45 (2)	96	100 (9)
CaCl <sub>2</sub>	0.45 (2)	40	79 (71)
FeCl <sub>3</sub>	0.032 (1)	82	89 (9)
CoCl <sub>3</sub>	0.032 (1)	73	78 (8)
NiCl <sub>2</sub>	0.032 (1)	71	83 (8.5)
CuCl <sub>2</sub>	0.032 (1)	86	100 (10)
MgCl <sub>2</sub> +LiCl	0.45 (2) + 0.85 (2)	99	99 (6)
MgCl <sub>2</sub> +NaCl	0.45 (2) + 0.85 (2)	82	93 (10)
MgCl <sub>2</sub> +NaCl	0.45 (1) + 0.85 (1)	100	100 (9)
MgCl <sub>2</sub> +KCl	0.45 (2) + 0.85 (2)	99	99 (5)
MgCl <sub>2</sub> +NH <sub>4</sub> Cl	0.45 (1) + 0.85 (1)	100	100 (2)
1	2	3	4
MgCl <sub>2</sub> +FeCl <sub>3</sub>	0.85 (2) + 0.032 (5)	65	83 (14)
MgCl <sub>2</sub> +CoCl <sub>2</sub>	0.85 (2) + 0.032 (5)	62	97 (24)

MgCl <sub>2</sub> +NiCl <sub>2</sub>	0.85 (2) + 0.032 (5)	67	95 (23)
MgCl <sub>2</sub> +CuCl <sub>2</sub>	0.85 (2) + 0.032 (5)	95	96 (6)
MgCl <sub>2</sub> +CuCl <sub>2</sub>	0.85 (1) + 0.032 (1)	100	100 (3.5)

Recently, CoCl<sub>2</sub> [34] and AlCl<sub>3</sub> [35] solutions were also tested as reaction mediums for hydrolysis of MgH<sub>2</sub>. The increase in CoCl<sub>2</sub> and AlCl<sub>3</sub> concentration resulted in an improved reaction kinetics and the maximum generation performance was obtained by using 6.25 wt.% CoCl<sub>2</sub> and 0.5 M AlCl<sub>3</sub> concentrated solutions. The improved hydrolysis performance is attributed to the large amounts of H<sup>+</sup> produced by the Al<sup>3+</sup> and Co<sup>2+</sup> hydrolysis that along with the Cl<sup>-</sup> pitting corrosion could contribute to destroying the Mg(OH)<sub>2</sub> layer wrapped on the surface of MgH<sub>2</sub>.

The influence of MgCl<sub>2</sub> and CaCl<sub>2</sub> salts on the hydrolysis of the hydrogenated 30 wt.% Ca–Mg alloy was investigated in [36]. Composites with various MgCl<sub>2</sub> and CaCl<sub>2</sub> content were obtained by ball milling for 0.5 h and were composed of Mg, MgH<sub>2</sub>, and Ca<sub>4</sub>Mg<sub>3</sub>H<sub>14</sub> phases, further to the chlorides. The hydrogen yields of the composites with MgCl<sub>2</sub> additive, in which the highest value is 1002 mL/g within 1 h, are lower than that of pure Ca–Mg alloy (1113 mL/g within 1 h). The authors attributed this effect to the displacement reaction and the common ion effect of Mg<sup>2+</sup>. However, composites with CaCl<sub>2</sub> chloride showed better hydrogen generation performances during the hydrolysis process. Moreover, with the increase of CaCl<sub>2</sub> content, the conversion rates of the composites also become higher due to the leaching and exothermic dissolution of CaCl<sub>2</sub>, which contributes to the formation of the fresh reactive material surfaces and disintegration of the passive layer. The hydrolysis performance of the hydrogenated 30 wt.% Ca–Mg alloy can be further improved by ball-milling with NH<sub>4</sub>Cl, as it was shown by the same group of investigators [37]. The hydrogenated Ca–Mg /5 wt.% NH<sub>4</sub>Cl composite has the best hydrolysis properties, generating 720 mL/g hydrogen in 1 min. The improved performance was explained by: (1) reduced particle size after the ball milling with NH<sub>4</sub>Cl; (2) formation of a new reactive material surface during leaching of chlorides from the composite; (3) high affinity of NH<sub>4</sub><sup>+</sup> to OH<sup>-</sup> and formation of soluble NH<sub>3</sub>·H<sub>2</sub>O.

The effect of additives of different nature, namely AlCl<sub>3</sub>, ethylenediaminetetraacetic acid (EDTA), and TiC–2TiB<sub>2</sub>, on the hydrolysis of MgH<sub>2</sub> was investigated in our earlier study [38]. It was found that MgH<sub>2</sub> + 5 wt.% EDTA unfortunately demonstrates the lowest

reactivity among the tested materials and produces only 176 mL/g H<sub>2</sub> in 10 min. The most probable reason for such a decreased efficiency is an interaction of MgH<sub>2</sub> with EDTA during the ball milling, which leads to the formation of magnesium salts and reduces the amount of highly active MgH<sub>2</sub> nanoparticles. As the result, only a small volume of MgH<sub>2</sub> can generate hydrogen during the hydrolysis, while the formed salts do not contribute to the hydrogen yield. Pure MgH<sub>2</sub> and MgH<sub>2</sub> + 5 wt.% TiC–2TiB<sub>2</sub> composite demonstrate a much improved hydrolysis performance (309–317 mL/g of hydrogen yield and 16.8–17.2% of the conversion rate after 10 min). However, still poor hydrolysis kinetics is attributed to the formation of a poorly soluble in water Mg(OH)<sub>2</sub> layer on the surface of MgH<sub>2</sub> particles, while the addition of 5 wt.% TiC–2TiB<sub>2</sub> does not contribute to the hydrolysis reaction probably due to non-optimized synthesis parameters. The maximum hydrogen yield of 557 mL/g MgH<sub>2</sub> and conversion rate of 30.3% were observed for MgH<sub>2</sub> + 5 wt.% AlCl<sub>3</sub> composition after 10 min of hydrolysis, which can be attributed to the destabilization of the Mg(OH)<sub>2</sub> layer by chlorine ions.

#### 2.4. Hydrolysis of MgH<sub>2</sub>-based materials with surfactant additives

The hydrolysis efficiency can be improved not only by adding different catalysts (acids, halides, oxides, etc.) but also by adjusting reaction conditions such as temperature, precursor's size, stirring, ultrasonic irradiation, etc. Recently, Chen et al. [39] investigated the effect of various surfactants on the hydrogen generation by hydrolysis of MgH<sub>2</sub> in water. It is known that surfactants can change the surface energy by forming an adsorbed layer with a certain orientation at the solid-liquid interface, and thus can influence the reaction kinetics. It was found that the addition of surfactants reduces the surface tension of the liquid, improves the wetting effect of the liquid to the MgH<sub>2</sub>, and increases the hydrogen yield. However, with the addition of surfactants, the reaction system is more prone to the formation of foam, limiting the release of hydrogen and thus reducing the efficiency of hydrogen generation. Moreover, different surfactants have variable effects on hydrogen generation. The hydrogen generation capacity from high to low is as follows: tetrapropylammonium bromide (TPABr), sodium dodecyl benzene sulfonate (SDBS), Ecosol 507, octadecyl trimethyl ammonium chloride (OTAC), sodium alcohol ether sulfate (AES), and fatty methyl ester sulfonate (FMES-70). The best

performance was observed when the ratio of  $MgH_2$  to TPABr was 5:1, and in this case the hydrogen generation increased by 52% as compared to the one without surfactants (after hydrolysis for 100 s). Due to the adsorptive effect of TPABr, it inhibits the formation of a passivation layer and prolongs the time for  $Mg(OH)_2$  to reach the critical in size volume. In addition, the reduced surface energy weakens the interaction among the particles and prevents their agglomeration. The surfactants can also change the morphology of  $Mg(OH)_2$ , which forms a three-dimensional stacking to produce a discontinuous layered structure that improves the continuity of the hydrolysis reaction.

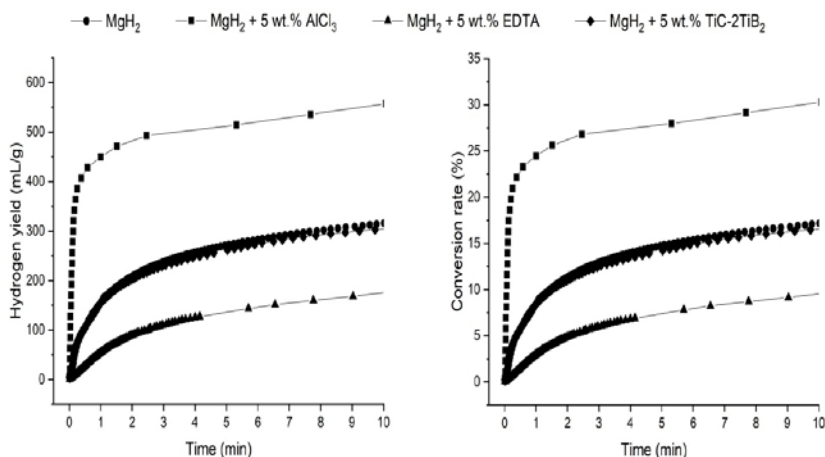


Fig. 1. Hydrogen yield (a) and conversion rate (b) for the  $MgH_2$  composites [38].

### 2.5. Summary of the main observations and regularities of the hydrolysis of $MgH_2$ -based materials

The main features of the hydrolysis performance of the  $MgH_2$ -based materials are summarized in Table 2.

Table 2 – Hydrolysis performance of  $MgH_2$ -based materials

Materials	Solution	Hydrogen conversion yield (%)	Hydrogen generation rate (mL/g) in 5 min	Activation energy (kJ/mol)	Ref.

1	2	3	4	5	6
MgH <sub>2</sub> - 5 wt.% C	Water	52.5% in 60 min	416	43.4	[31]
MgH <sub>2</sub> - 5 wt.% C- 5 wt.% Fe <sub>2</sub> O <sub>3</sub>	Water	62.8% in 60 min	468	36.92	
MgH <sub>2</sub> - 5 wt.% Ge	30 wt.% acetic acid	100% in 1 min	-	-	[25]
H- 10 wt.% Mg- 10 wt.% TiO <sub>2</sub>	0.1M MgCl <sub>2</sub>	93.7% in 60 min	~400	45.14	[30]
H- 10 wt.% Mg- 10 wt.% Al <sub>2</sub> O <sub>3</sub>		93.3% in 60 min	~390	51.06	
H- 10 wt.% Mg- 10 wt.% Fe <sub>2</sub> O <sub>3</sub>		85.1% in 60 min	~470	47.62	
H-MgLi	Deionized water	-	734	-	[27]
	0.1M MgCl <sub>2</sub>	-	1247	-	
	0.5M MgCl <sub>2</sub>	-	1263	-	
	1M MgCl <sub>2</sub>	90% in 30 min	1542	24.6	
MgH <sub>2</sub>	0.1M AlCl <sub>3</sub>	~60% in 60 min	~450	34.68	[35]
	0.5M AlCl <sub>3</sub>	~100% in 60 min	~950	21.64	
H- 30wt.% Ca-Mg	Water	55.9% in 60 min	~540	-	[37]
1	2	3	4	5	6
H- 30wt.% Ca-Mg -3% NH <sub>4</sub> Cl	Water	61% in 60 min	~690	-	[37]

H- 30wt.% Ca-Mg -5% NH <sub>4</sub> Cl		67% in 60 min	~830	-		
H- 30wt.% Ca-Mg -7% NH <sub>4</sub> Cl		65.9% in 60 min	~820	-		
H- 30wt.% Ca-Mg -10% NH <sub>4</sub> Cl		66.5% in 60 min	~800	-		
MgH <sub>2</sub>	0.1M MgCl <sub>2</sub>	63.7% in 60 min	~400	54.1±2.5	[24]	
H-Mg- 10 wt.% In		92% in 60 min	~540	43.4±1.1		
H-Mg- 5 wt.% Ag		90.7% in 60 min	~480	59.6±2.7		
MgH <sub>2</sub>	Deionized water		377.0	-	[32]	
MgH <sub>2</sub> + 10wt.% MgO			433.0	-		
MgH <sub>2</sub> + 10wt.% Al <sub>2</sub> O <sub>3</sub>			432.4	-		
MgH <sub>2</sub> + 10wt.% CaO			421.0	-		
MgH <sub>2</sub> + 10wt.% Mg(OH) <sub>2</sub>			407.2	-		
MgH <sub>2</sub> + 10wt.% Al(OH) <sub>3</sub>			357.3	-		
MgH <sub>2</sub> + 10wt.% Ca(OH) <sub>2</sub>			340.0	-		
MgH <sub>2</sub> + 10wt.% CoCl <sub>2</sub>			~88% in 60 min	1481.7		17.59
1		2	3	4		5
MgH <sub>2</sub> + 10wt.% NiCl <sub>2</sub>	Deionized water		1496.1	-	[32]	

MgH <sub>2</sub> + 10wt.% CuCl <sub>2</sub>			1472.1	-	
MgH <sub>2</sub> + 10wt.% MgCl <sub>2</sub>			1554.6	-	
MgH <sub>2</sub> + 10wt.% NaCl			540.1	-	
MgH <sub>2</sub> + 10wt.% KCl			590.2	-	
MgH <sub>2</sub> + 10wt.% CaCl <sub>2</sub>			604.5	-	
H-CaMg <sub>2</sub>		~72% in 1 min	800	-	[26]
H-CaMg <sub>1.9</sub> Ni <sub>0.1</sub>		~87% in 5 min	968	32.9	
H- 30wt.%Ca-Mg	Water	74.5% in 60 min	~600	-	[36]
H- 30wt.%Ca-Mg -5% MgCl <sub>2</sub>		77.4% in 60 min	~720	-	
H- 30wt.%Ca-Mg -10% MgCl <sub>2</sub>		70.8% in 60 min	~560	-	
H- 30wt.%Ca-Mg -15% MgCl <sub>2</sub>		69% in 60 min	~510	-	
H- 30wt.%Ca-Mg -20% MgCl <sub>2</sub>		70.3% in 60 min	~550	-	
H- 30wt.%Ca-Mg -5% CaCl <sub>2</sub>		83.2% in 60 min	~750	-	
H- 30wt.%Ca-Mg -10% CaCl <sub>2</sub>		81.8% in 60 min	~710	-	
H- 30wt.%Ca-Mg -15% CaCl <sub>2</sub>		81.4% in 60 min	~690	-	
1		2	3	4	

H- 30wt.% Ca-Mg -20% CaCl <sub>2</sub>	Water	76.9% in 60 min	~580	-	[36]
H-Mg - 10 wt.% Ni	3.5 wt.% NaCl	97% in 30 min	-	30.19	[17]
H-Mg - 10 wt.% Fe		81% in 30 min	-	36.09	
H-Mg - 10 wt.% Al		45% in 30 min	-	-	
H-Mg - 10 wt.% Nb <sub>2</sub> O <sub>5</sub>		57.3% in 30 min	-	31.46	
H-Mg - 10 wt.% V <sub>2</sub> O <sub>5</sub>		52.5% in 30 min	-	-	
MgH <sub>2</sub>		Distilled water	17.2% in 10 min	272	
MgH <sub>2</sub> + 5 wt.% TiC- 2TiB <sub>2</sub>	16.8% in 10 min		260	-	
MgH <sub>2</sub> + 5 wt.% AlCl <sub>3</sub>	30.3% in 10 min		512	-	
MgH <sub>2</sub> + 5 wt.% EDTA	9.6% in 10 min		140	-	
MgH <sub>2</sub>	19% in 10 min		335	-	This study
MgH <sub>2</sub> + 5 wt.% MgCl <sub>2</sub>	33.5% in 10 min		616	-	
MgH <sub>2</sub> + 5 wt.% MgCl <sub>2</sub> + 1 wt.% TiC- 2TiB <sub>2</sub>	34.4% in 10 min		633	-	

### 3. Experimental studies

The nanocrystalline magnesium hydride powder (sample S1) was prepared by a reactive ball milling of Mg powder (Fluka, 99.8%, grit, 50–150 mesh) in hydrogen gas. The milling was performed in a Retsch PM 100 ball mill using high-pressure milling vial commercialized by Evicomagnetics GmbH filled with hydrogen gas ( $P = 80$  bar H<sub>2</sub>) and stainless steel balls of 10 mm in diameter each, at a rotation speed of 400 rpm, with a ball-to-powder mass ratio of 65:1. The milling was conducted in two cycles, 90 min milling time and 90 min rest each, i.e. total milling time of

180 min. The handling of the samples was carried out in a glove box filled with purified argon gas.

In order to study the effect of preparation procedures on the hydrolysis of  $\text{MgH}_2 - \text{MgCl}_2$  composites, the samples were prepared in different ways:

1) mixing of preliminary synthesized  $\text{MgH}_2$  with 5 wt.%  $\text{MgCl}_2$  in an agate mortar for 30 min (sample S2);

2) simultaneous hydrogenation of Mg and its milling with 5 wt.%  $\text{MgCl}_2$  in a ball mill for 180 min (sample S3);

3) milling of a preliminary synthesized  $\text{MgH}_2$  with 5 wt.%  $\text{MgCl}_2$  in a ball mill for 30 min (sample S4);

4) milling of a preliminary obtained  $\text{MgH}_2$  with 5 wt.%  $\text{MgCl}_2$  and 1 wt.%  $\text{TiC}-2\text{TiB}_2$  in a ball mill for 30 min (sample S5).

Ball milling of preliminary synthesized  $\text{MgH}_2$  with additives was performed in  $\text{H}_2$  at 400 rpm for 30 min, while a hand milling in the agate mortar was conducted in a glove box filled with a purified Ar.

The hydrogen generation during the hydrolysis reaction was monitored by using a water replacement method, by using a homemade setup that consists of a reaction volume and gas collecting/measuring components. The reaction part is a 500 mL four-neck glass flask with openings for water addition, insertion of a thermometer, Ar purge gas, and  $\text{H}_2$  removal. The reaction part is connected by a silicone tube to the collecting/measuring part, which consists of gas washing bottle, beaker, and electronic balance. The hydrogen drains the water from the gas washing bottle to the beaker placed on the electronic balance. The amount of hydrogen is estimated by the measurements of the mass of the replaced water.

The samples in a form of powders were placed into the flask with subsequent system sealing. After that, the apparatus was purged with argon gas for 5 min, and the flask was filled with distilled water from the pressure-equalizing funnel to start the hydrolysis reaction. All experiments were carried out at room temperature and atmospheric pressure.

The hydrogen generation or conversion yield (%) was defined as the ratio between the actual amount of the produced hydrogen and the

theoretical amount that should be released, assuming a completeness of the reaction of the hydride with water.

X-ray powder diffraction (XRD) measurements were performed on a DRON-3 diffractometer with Cu  $K\alpha$  radiation ( $\lambda=1.5406 \text{ \AA}$ ) in the  $2\theta$  range from  $20^\circ$  to  $80^\circ$  with a scanning rate of  $0.15^\circ/\text{min}$  and a step size of  $0,01^\circ$ .

#### 4. Results and discussion

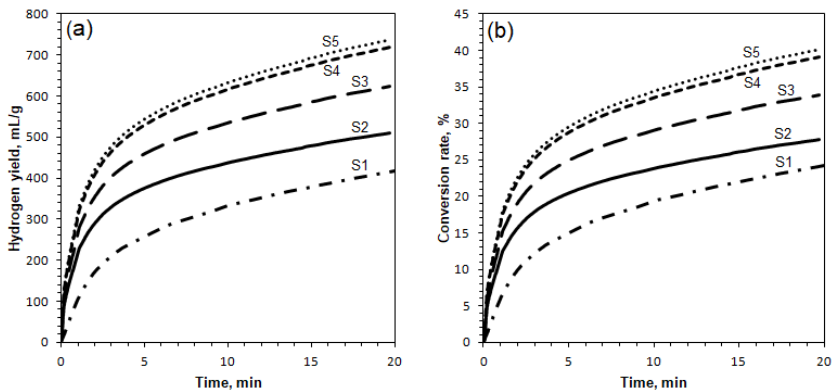
The XRD analysis of magnesium hydride sample prepared by reactive ball milling of Mg powder under hydrogen pressure reveals that at the selected synthesis parameters a complete hydrogenation of magnesium occurs resulting in the formation of two polymorphic modifications of  $\text{MgH}_2$ , namely,  $\beta\text{-MgH}_2$  and a high-pressure modification  $\gamma\text{-MgH}_2$ . The broad diffraction peaks of the synthesized hydride indicate that the material is nanocrystalline. No Mg peaks were observed in the XRD pattern of the prepared  $\text{MgH}_2$ .

The hydrogen generation properties by hydrolysis of all samples were studied at room temperature using a distilled water, and corresponding hydrogen generation and conversion rate curves are shown in Fig. 2. According to the Fig. 2a, the hydrolysis reaction of pure  $\text{MgH}_2$  (sample S1) is rather sluggish, delivering only 335 mL/g and 419 mL/g hydrogen, while the conversion rate of the hydrolysis reaction reached  $\sim 19\%$  and  $\sim 24\%$  within 10 min and 20 min, respectively. This slow hydrogen generation rate is not surprising, since the reaction between  $\text{MgH}_2$  and water is rapidly interrupted due to the formation of a passive  $\text{Mg(OH)}_2$  layer on the surface of the  $\text{MgH}_2$  particles. The formed  $\text{Mg(OH)}_2$  layer has low solubility in water and prevents further contact between the water and the hydride.

The hydrolysis kinetics and hydrogen yield of  $\text{MgH}_2$  can be increased by addition of the chloride salts, such as  $\text{MgCl}_2$ .  $\text{MgCl}_2$  is an acidic chloride, and thus, it increases content of  $\text{H}^+$ , making the corresponding aqueous solution weakly acidic. A large amount of  $\text{Cl}^-$  and  $\text{H}^+$  ions derived from the acid chloride aqueous solution can affect the  $\text{Mg(OH)}_2$  layer via both pitting and  $\text{H}^+$  corrosion, therefore creating more channels for the reaction between  $\text{MgH}_2$  and water [32]. In the case of the

MgH<sub>2</sub> + 5 wt.% MgCl<sub>2</sub> composite that was prepared by hand mixing of the previously synthesized MgH<sub>2</sub> and MgCl<sub>2</sub> in an agate mortar for 30 min (sample S2), the hydrolysis performance improved for about 32% as compared to the individual MgH<sub>2</sub> (Fig. 2). The hydrogen yield of 512 mL/g and conversion rate of 28.8% were observed for the prepared sample after 20 min of hydrolysis (Fig. 2). The insignificant improvement of the hydrolysis performance can be attributed to the insufficient efficiency of the hand mixing by using a mortar. As the result, MgCl<sub>2</sub> was inhomogeneously distributed in the MgH<sub>2</sub> powder with only a small fraction of MgCl<sub>2</sub> having a good contact with the MgH<sub>2</sub> particles, and thus having a limited contribution to the destabilization of the Mg(OH)<sub>2</sub> layer.

Fig. 2. Kinetic curves of hydrogen yield (a) and conversion rate (b) for MgH<sub>2</sub> – MgCl<sub>2</sub> composites prepared by various techniques.



When the MgH<sub>2</sub> + 5 wt.% MgCl<sub>2</sub> composite (sample S3) was prepared by a simultaneous hydrogenation of Mg and its mixing with 5 wt.% MgCl<sub>2</sub> in a ball mill for 180 min, both hydrogen yield and conversion rate further increased, reaching about 623 mL/g H<sub>2</sub> and 34% in 20 min, respectively (Fig. 2). The enhanced hydrolysis performance is attributed to the homogeneous distribution of MgCl<sub>2</sub> salt over the nanocrystalline MgH<sub>2</sub> particles after the reactive ball milling.

However, the MgH<sub>2</sub> + 5 wt.% MgCl<sub>2</sub> composite (sample S4) that was obtained by mixing a preliminary synthesized MgH<sub>2</sub> with 5 wt.%

MgCl<sub>2</sub> in a planetary ball mill for 30 min showed a much higher hydrolysis efficiency, which was about 15% higher than that of the sample prepared by simultaneous hydrogenation of Mg and its milling with MgCl<sub>2</sub>. In this case the hydrogen yield of 719 mL/g and a conversion rate of 39.1% were obtained after 20 min of hydrolysis (Fig. 2). In our opinion such improvement of the hydrolysis process can be a result of the "mild" conditions that were realized during the ball milling of preliminary synthesized MgH<sub>2</sub> and MgCl<sub>2</sub> powders, and can provide a homogeneous distribution of the materials after 30 min of the milling. In contrast, during the simultaneous hydrogenation of Mg and its milling with MgCl<sub>2</sub>, the latter can affect the hydrogenation process and/or react with MgH<sub>2</sub> hydride, leading to the reduced hydrogen generation.

The reactivity of the MgH<sub>2</sub> particles with water can be increased by adding hard and brittle powdered materials that improve the efficiency of the ball milling process by decreasing the particle size and by creating more microstructural defects. In this respect, the TiC–2TiB<sub>2</sub> composite that was previously studied by us as an additive to MgH<sub>2</sub> [38], can be used for this purpose. However, since the TiC–2TiB<sub>2</sub> additive does not participate in the hydrolysis reaction either as a raw material or as a part of a micro-galvanic cell, its amount was limited to 1 wt.%. The hydrolysis performance of the MgH<sub>2</sub> + 5 wt.% MgCl<sub>2</sub> + 1 wt.% TiC–2TiB<sub>2</sub> composite (sample S5) prepared by mixing previously hydrogenated MgH<sub>2</sub> with 5 wt.% MgCl<sub>2</sub> + 1 wt.% TiC–2TiB<sub>2</sub> powders in a ball mill for 30 min, is shown in Fig. 2. From Fig. 2, it can be seen that prepared composite demonstrates the highest reactivity among the tested materials and produces 738 mL/g hydrogen in 20 min, which corresponds to the conversion rate of 40.2%. The hydrolysis performance improved by about 5% in comparison with that of the material without 1 wt.% TiC–2TiB<sub>2</sub> additive. Thus, the combined effect of the Cl<sup>-</sup> and H<sup>+</sup> ions from chloride aqueous solution and grinding additive is responsible for a significant enhancement of the hydrolysis reaction.

## Conclusions

In the present work we have reviewed recent reference publications on the hydrolysis of MgH<sub>2</sub>-based materials and current approaches to enhance the hydrolysis performance when utilizing metals, oxides, hydroxides and halides as additives, as well as surfactants. We summarized the recent advances in the work on the hydrolysis of the composites based on magnesium hydride where the most distinct improvements were observed for the various salt additives while the reaction rate appears to depend more on the additive type rather than its concentration. In this study we explored the influence of the preparation procedures on the hydrolysis of MgH<sub>2</sub> – MgCl<sub>2</sub> composites, which suggests that milling of MgH<sub>2</sub>, preliminary obtained by mechano-chemical synthesis, with the addition of MgCl<sub>2</sub> is as a preferred route to achieve advanced hydrolysis performance of the composite.

### Acknowledgments

This work was supported by the NATO Programme "Science for Peace and Security" (Project G5233 "Portable Energy Supply").

### References

- [1] Marbán G., Valdés-Solís T. Towards the hydrogen economy? *Int. J. Hydrogen Energy*, 2007, vol. 32, Issue 12, pp. 1625–1637. <https://doi.org/10.1016/j.ijhydene.2006.12.017>.
- [2] Abdin Z., Zafaranloo A., A. Rafiee, Merida W., Lipinski W., Khalilpour K.R. Hydrogen as an energy vector, *Renew. Sustain. Energy Rev*, 2020, vol. 120, pp. 109620. <https://doi.org/10.1016/j.rser.2019.109620>.
- [3] Eberle U., Felderhoff M., Schuth F. Chemical and physical solutions for hydrogen storage, *Angew. Chem. Int. Ed*, 2009. vol. 48, pp. 6608–6630. <https://doi.org/10.1002/anie.200806293>.
- [4] Bellosta von Colbe J., Ares J.-R., Barale J., Baricco M., Buckley C., Capurso G., Gallandat N., Grant D.M., Guzik M.N., Jacob I., Jensen E.H., Jensen T., Jepsen J., Klassen T., Lototsky M.V., Manickam K., Montone

A., Puzskiel J., Sartori S., Sheppard D.A., Stuart A., Walker G., Webb C.J., Yang H., Yartys V., Züttel A., Dornheim M. Application of hydrides in hydrogen storage and compression: Achievements, outlook and perspectives, *Int. J. Hydrogen Energy*, 2019, vol. 44, Issue 15, pp. 7780–7808.

<https://doi.org/10.1016/j.ijhydene.2019.01.104>.

[5] Tegel M., Schone S., Kieback B., Röntzsch L. An efficient hydrolysis of  $MgH_2$ -based materials, *Int. J. Hydrogen Energy*, 2017, vol. 42, Issue 4, pp. 2167–2176.

<https://doi.org/10.1016/j.ijhydene.2016.09.084>.

[6] Ropp R.C. *Encyclopedia of the Alkaline Earth Compounds*, Elsevier, 2013. 1216 p.

[7] Hirscher M., Yartys V.A., Baricco M. *et.al.*, Materials for hydrogen-based energy storage – past, recent progress and future outlook, *J. Alloys Compd.*, 2020, vol. 827, pp. 153548.

<https://doi.org/10.1016/j.jallcom.2019.153548>.

[8] Yartys V.A., Lototsky M.V., Akiba E. *et.al.*, Magnesium based materials for hydrogen based energy storage: Past, present and future. *Int. J. Hydrogen Energy*, 2019, vol. 44, Issue 15, pp. 7809–7859.

<https://doi.org/10.1016/j.ijhydene.2018.12.212>.

[9] Crivello J.-C., Dam B., Denys R.V. *et.al.* Review of magnesium hydride-based materials: development and optimization, *Appl. Phys. A*, 2016, vol. 122, No. 97, pp. 1–20.

<https://doi.org/10.1007/s00339-016-9602-0>.

[10] Sadhasivam T., Kim H.-T., Jung S., Roh S.-H., Park J.-H., Jung H.-Y. Dimensional effects of nanostructured Mg/MgH<sub>2</sub> for hydrogen storage applications: A review. *Renewable Sustainable Energy Rev.*, 2017, vol. 27, pp. 523–534.

<https://doi.org/10.1016/j.rser.2017.01.107>.

[11] Wang Y., Wang Y. Recent advances in additive-enhanced magnesium hydride for hydrogen storage, *Prog. Nat. Sci.*, 2017, vol. 27, Issue 1, pp. 41–49. <https://doi.org/10.1016/j.pnsc.2016.12.016>.

[12] Sun Y., Shen C., Lai Q., Liu W., Wang D.-W., Aguey-Zinsou K.-F. Tailoring magnesium based materials for hydrogen storage through synthesis: Current state of the art. *Energy Storage Mater.*, 2018, vol. 10,

pp. 168–198. <https://doi.org/10.1016/j.ensm.2017.01.010>.

[13] Manilevich F.D., Pirskey Yu.K., Danil'tsev B.I., Kutsyi A.V., Yartys V.A. Studies of the hydrolysis of aluminum activated by additions of Ga–In–Sn eutectic alloy, bismuth, or antimony, *Mater. Sci.*, 2020, vol. 55, No. 4, pp. 536–547. <https://doi.org/10.1007/s11003-020-00336-x>.

[14] Hong S.-H., Kim H.-J., Song M.Y. Rate enhancement of hydrogen generation through the reaction of magnesium hydride with water by MgO addition and ball milling, *J. Ind. Eng. Chem.*, 2012, vol. 18, Issue 1, pp. 405–408. <https://doi.org/10.1016/j.jiec.2011.11.104>.

[15] Laversenne L., Goutaudier C., Chiriach R., Sigala C., Bonnetot B. Hydrogen storage in borohydrides: Comparison of hydrolysis conditions of LiBH<sub>4</sub>, NaBH<sub>4</sub> and KBH<sub>4</sub>. *J. Therm. Anal. Calorim.*, 2008, vol. 94, pp. 785–790. <https://doi.org/10.1007/s10973-008-9073-4>.

[16] Tayeh T., Awad A.S., Nakhl M., Zakhour M., Silvain J.-F., Bobet J.-L. Production of hydrogen from magnesium hydrides hydrolysis, *Int. J. Hydrogen Energy*, 2014, vol. 39. pp. 3109–3117. <https://doi.org/10.1016/j.ijhydene.2013.12.082>.

[17] Awad A.S., El-Asmar E., Tayeh T., Mauvy F., Nakhl M., Zakhour M., Bobet J.L. Effect of carbons (G and CFs), TM (Ni, Fe, and Al) and oxides (Nb<sub>2</sub>O<sub>5</sub> and V<sub>2</sub>O<sub>5</sub>) on hydrogen generation from ball milled Mg-based hydrolysis reaction for fuel cell, *Energy*, 2016, vol. 95, pp. 175–186. <https://doi.org/10.1016/j.energy.2015.12.004>.

[18] Zou M.S., Yang R.J., Guo X.Y., Huang H.T., He J.Y., Zhang P. The preparation of Mg-based hydro-reactive materials and their reactive properties in seawater, *Int. J. Hydrogen Energy*, 2011, vol. 36, Issue 11, pp. 6478–6483. <https://doi.org/10.1016/j.ijhydene.2011.02.108>.

[19] Li S., Gan D.-Y., Zhu Y.-F., Liu Y.-N., Zhang G., Li L.-Q. Influence of chloride salts on hydrogen generation via hydrolysis of MgH<sub>2</sub> prepared by hydriding combustion synthesis and mechanical milling, *Trans. Nonferrous Met. Soc. China*, 2017, vol. 27, pp. 562–568. [https://doi.org/10.1016/S1003-6326\(17\)60062-1](https://doi.org/10.1016/S1003-6326(17)60062-1).

[20] Huang J.M., Duan R.M., Ouyang L.Z., Wen Y.J., Wang H., Zhu M. The effect of particle size on hydrolysis properties of Mg<sub>3</sub>La hydrides, *Int. J. Hydrogen Energy*, 2014, vol. 39, Issue 25, pp. 13564–13568.

<https://doi.org/10.1016/j.ijhydene.2014.04.024>.

[21] Huang J.M., Ouyang L.Z., Wen Y.J., Wang H., Liu J.W., Chen Z.L., Zhu M. Improved hydrolysis properties of  $Mg_3RE$  hydrides alloyed with Ni. *Int. J. Hydrogen Energy*, 2014, vol. 39, Issue 13, pp. 6813–6818. <https://doi.org/10.1016/j.ijhydene.2014.02.155>.

[22] Xiao Y., Wu C.L., Wu H.W., Chen Y.G. Hydrogen generation by  $CaH_2$ -induced hydrolysis of  $Mg_{17}Al_{12}$  hydride, *Int. J. Hydrogen Energy*, 2011, vol. 36, Issue 24, pp. 15698–15703.

<https://doi.org/10.1016/j.ijhydene.2011.09.022>.

[23] Liu P.P., Wu H.W., Wu C.L., Chen Y.G., Xu Y.M., Wang X.L., Zhang Y.B. Microstructure characteristics and hydrolysis mechanism of Mg-Ca alloy hydrides for hydrogen generation, *Int. J. Hydrogen Energy*, 2015, vol. 40, Issue 10, pp. 3806–3812.

<https://doi.org/10.1016/j.ijhydene.2015.01.105>.

[24] Mao J.W., Huang T.P., Panda S., Zou J.X., Ding W.J. Direct observations of diffusion controlled microstructure transition in Mg-In/Mg-Ag ultrafine particles with enhanced hydrogen storage and hydrolysis properties, *Chem. Eng. J.*, 2021, vol. 418, pp. 129301. <https://doi.org/10.1016/j.cej.2021.129301>.

[25] Adeniran J.A., Akbarzadeh R., Lototskyy M., Nyallang Nyamsi S., Olorundare O.F., Akinlabi E.T., Jen T.C. Phase-structural and morphological features, dehydrogenation/re-hydrogenation performance and hydrolysis of nanocomposites prepared by ball milling of  $MgH_2$  with germanium, *Int. J. Hydrogen Energy*, 2019, vol. 44, Issue 41, pp. 23160–23171. <https://doi.org/10.1016/j.ijhydene.2019.06.119>.

[26] Ma M.L., Duan R.M., Ouyang L.Z. Zhu X.K., Peng C.H., Zhu M. Hydrogen generation via hydrolysis of H- $CaMg_2$  and H- $CaMg_{1.9}Ni_{0.1}$ , *Int. J. Hydrogen Energy*, 2017, vol. 42, Issue 35. P. 22312–22317. <https://doi.org/10.1016/j.ijhydene.2017.05.159>.

[27] Jiang J., Ouyang L.Z., Wang H., Liu J.W., Shao H.Y., Zhu M. Controllable hydrolysis performance of MgLi alloys and the hydrides, *ChemPhysChem.*, 2019, vol. 20, Issue 10, pp. 1316–1324. <https://doi.org/10.1002/cphc.201900058>.

- [28] Naseem K., Zhong H., Wang H., Ouyang L.Z., Zhu M. Promoting hydrogen generation via co-hydrolysis of Al and  $\text{MgH}_2$  catalyzed by Mo and  $\text{B}_2\text{O}_3$ , *J. Alloys Compd.*, 2021, vol. 888, pp. 161485. <https://doi.org/10.1016/j.jallcom.2021.161485>.
- [29] Hong S.H., Kim H.J., Song M.Y. Rate enhancement of hydrogen generation through the reaction of magnesium hydride with water by MgO addition and ball milling, *J. Ind. Eng. Chem.*, 2012, vol. 18, Issue 1, pp. 405–408. <https://doi.org/10.1016/j.jiec.2011.11.104>.
- [30] Yang B., Zou J.X., Huang T.P., Mao J.F., Zeng X.Q., Ding W.J. Enhanced hydrogenation and hydrolysis properties of core-shell structured Mg- $\text{MO}_x$  (M=Al, Ti and Fe) nanocomposites prepared by arc plasma method, *Chem. Eng. J.*, 2019, vol. 371, pp. 233–243. <https://doi.org/10.1016/j.cej.2019.04.046>.
- [31] Yang K., Qin H.Y., Lv J.N., Yu R.J., Chen X., Zhao Z.D., Li Y.J., Zhang F., Xia X.C., Fu Q., Wang M. The effect of graphite and  $\text{Fe}_2\text{O}_3$  addition on hydrolysis kinetics of Mg-based hydrogen storage materials, *Int. J. Photoenergy.*, 2021, vol. 2021, pp. 6651541. <https://doi.org/10.1155/2021/6651541>.
- [32] Zhou C., Zhang J.G., Zhu Y.F., Liu Y., Li L.Q. Controllable hydrogen generation behavior by hydrolysis of  $\text{MgH}_2$ -based materials, *J. Power Sources*, 2021, vol. 494, pp. 229726. <https://doi.org/10.1016/j.jpowsour.2021.229726>.
- [33] Sevastyanova L.G., Klyamkin S.N., Bulychev B.M. Generation of hydrogen from magnesium hydride oxidation in water in presence of halides. *Int. J. Hydrogen Energy*, 2020, vol. 45, Issue 4, pp. 3046–3052. <https://doi.org/10.1016/j.ijhydene.2019.11.226>.
- [34] Coşkuner Filiz B. Investigation of the reaction mechanism of the hydrolysis of  $\text{MgH}_2$  in  $\text{CoCl}_2$  solutions under various kinetic conditions, *Reac. Kinet. Mech. Cat.*, 2021, vol. 132, pp. 93–109. <https://doi.org/10.1007/s11144-020-01923-4>.
- [35] Gan D.Y., Liu Y., Zhang J.G., Zhang Y., Cao. C.T., Zhu Y.F., Li L.Q. Kinetic performance of hydrogen generation enhanced by  $\text{AlCl}_3$  via hydrolysis of  $\text{MgH}_2$  prepared by hydriding combustion synthesis, *Int. J.*

*Hydrogen Energy*, 2018, vol. 43, Issue 22, pp. 10232– 10239.  
<https://doi.org/10.1016/j.ijhydene.2018.04.119>.

[36] Li J.F., Liu P.P., Wu C.L., Chen Y.G. Common ion effect in the hydrolysis reaction of Mg–Ca alloy hydride-salt composites, *Int. J. Hydrogen Energy*, 2017, vol. 42, Issue 2, pp. 1429– 1435.  
<https://doi.org/10.1016/j.ijhydene.2016.06.006>.

[37] Zhong S.A., Wu C.L., Chen Y.G., Feng Z., Zhao Y., Xia Y.T. Enhanced hydrolysis performance and the air-stability of Mg–Ca hydride-chloride composites, *J. Alloys Compd.*, 2019, vol. 792, pp. 869–877.  
<https://doi.org/10.1016/j.jallcom.2019.03.394>.

[38] Korablov D.S., Bezdorozhev O.V., Gierlotka S., Yartys V.A., Solonin Yu.M. Effect of various additives on the hydrolysis performance of nanostructured MgH<sub>2</sub> synthesized by high-energy ball milling in hydrogen, *Powder Metall. Met. Ceram.*, 2021, vol. 59, pp. 483–490.  
<https://doi.org/10.1007/s11106-021-00193-6>.

[39] Chen et al. Chen Y.Y., Wang M., Guan F.G., Yu R.J., Zhang Y.Y., Qin H.Y., Chen X., Fu Q., Wang Z.Y. Study on hydrolysis of magnesium hydride by interface control, *Int. J. Photoenergy*, 2020, vol. 2020, pp. 8859770.  
<https://doi.org/10.1155/2020/8859770>.